Distributions of diffusion measures from a local mean-square displacement analysis

Amitabha Nandi,[1,2,*] Doris Heinrich,[3] and Benjamin Lindner[1,4]

[1]*Max-Planck Institut für Physik komplexer Systeme, Nöthnitzer Str. 38, 01187 Dresden, Germany*
[2]*Department of Molecular, Cellular and Developmental Biology, Yale University, New Haven, Connecticut 06520, USA*
[3]*Faculty of Physics, Center for NanoScience (CeNS), Ludwig-Maximilians-Universität, Geschwister-Scholl-Platz 1, 80539 Munich, Germany*
[4]*Bernstein Center for Computational Neuroscience Berlin, Institute of Physics, Humboldt University Berlin, Germany*

In cell biology, time-resolved fluctuation analysis of tracer particles has recently gained great importance. One such method is the local mean-square displacement (MSD) analysis, which provides an estimate of two parameters as functions of time: the exponent of growth of the MSD and the diffusion coefficient. Here, we study the joint and marginal distributions of these parameters for Brownian motion with Gaussian velocity fluctuations, including the cases of vanishing correlations (overdamped Brownian motion) and of a finite negative velocity correlation (as observed in intracellular motion). Numerically, we demonstrate that a small number of MSD points is optimal for the estimation of the diffusion measures. Motivated by this observation, we derive an analytic approximation for the joint and marginal probability densities of the exponent and diffusion coefficient for the special case of two MSD points. These analytical results show good agreement with numerical simulations for sufficiently large window sizes. Our results might promote better statistical analysis of intracellular motility.

I. INTRODUCTION

The analysis of single-particle-tracking experiments is important to reveal valuable information about intracellular transport processes and the complex dynamics of the cytoskeleton. Here, mean-square displacement (MSD) is often used to characterize intracellular transport phenomena. Organelles inside eukaryotic cells are transported in two ways (two motility modes): (i) pulled by molecular motors along intracellular filaments and (if not bound to a filament) (ii) pushed around by cytoskeletal components. Recent experimental [1,2] and theoretical papers [3] suggest that intracellular transport can be described as a combination of free (sub)diffusion and phases of active transport; for a more detailed picture, see the recent review in Ref. [4]. In most other cell types, tracer particles (comparable in size to organelles) switch stochastically between the two motility modes on a subsecond time scale, possibly optimized for the transport task at hand [3]. Such switchings cannot be resolved by a standard global MSD analysis, which extends over a time scale of seconds or longer.

Recently, a novel technique called the local MSD analysis has been introduced [1,2]. Here, the MSD is measured over a comparatively small averaging time window, and the resulting MSD curve is fitted to a power law,

$$\overline{\Delta R^2} \sim t^\alpha \qquad (1)$$

(details of the fitting procedure are discussed below), and the parameters of the fit are related to the diffusion coefficient and the exponent of MSD growth, respectively. In particular, the value of α defines the type of motion [5,6]: For α significantly below 1, the particle performs subdiffusion, whereas, α greater than 1 implies superdiffusion with the limiting ballistic case of $\alpha = 2$.

The values of diffusion coefficient and exponent are assigned to a reference point (preferably the midpoint) of the averaging time window; by sliding the window over the trajectory, one obtains (temporally) local information on the diffusive or transport behavior. Using the time series of the exponent α, one can distinguish typical phases of intracellular motion: phases of subdiffusion and phases of directed transport.

In general, even if the vesicle or bead is restricted to perform only one kind of motion, subdiffusion, for instance, the parameters resulting from the local MSD algorithm will be statistically distributed. Put differently, because we use a temporal finite-size average of the trajectories, the resulting time series for the diffusion coefficient and the exponent are still stochastic. The probability densities of these exponents of growth and of the diffusion coefficient (related to the prefactor of the fitting law A) will be shaped not only by the properties of the cytoplasm, but also by the MSD algorithm itself. When exploring the properties of the cytoplasm, it is certainly desirable to entangle and to separate these two factors. A good starting point in this regard seems to be the calculation of the statistics for model systems, such as a simple Brownian motion. In a recent paper, we showed that a simple model with correlated Gaussian velocity fluctuations could reproduce the statistics of the MSD parameters of experimental data on intracellular bead motion [7]. Here, we explore this model theoretically and derive approximate expressions for the probability densities of the motion parameters. More specifically, we calculate the joint and marginal densities for the MSD exponent and effective diffusion coefficient. We start with the comparatively simple case of an overdamped Brownian motion (uncorrelated Gaussian velocity fluctuations) and then derive formulas for the more interesting case of a correlated Gaussian velocity leading to transient subdiffusion. For the latter case, we also compare the local MSD analysis to the characteristics of subdiffusion as seen in the long-time MSD average. Our results may contribute to a proper interpretation of the local MSD analysis as it is used by experimental groups.

Our paper is organized as follows. First, we discuss the local MSD algorithm in detail. Then, we present our stochastic

*amitabha.nandi@yale.edu

model: a random motion with Gaussian velocity fluctuations, the correlation function of which is given. We discuss results for this model for two specific choices of the correlation function: (i) uncorrelated velocity noise, corresponding to an overdamped Brownian motion and (ii) a negative exponentially decaying correlation [antipersistent motion (AP)] similar to that found in experiments on intracellular motion. We derive and compare approximation formulas for the case of two MSD points to numerical simulations. We also explore using numerical simulations, the more involved case of more than two MSD points and discuss our results in comparison to the exact MSD obtained by a long-time average. The paper concludes with a summary and discussion of our findings. Details of the analytical derivations are discussed in the Appendix.

II. LOCAL MSD ALGORITHM

The conventional method of analyzing experimentally recorded trajectories is based on estimates of the MSD. For a trajectory of time length T, the MSD is approximately given by

$$\overline{\Delta R_t^2(\tau)} = \frac{1}{T-\tau} \int_0^{T-\tau} ds [\mathbf{R}(t+s+\tau) - \mathbf{R}(t+s)]^2. \quad (2)$$

For the case of Brownian motion, the time average shown in Eq. (2) can be replaced by an ensemble average taken over a large number of trajectories (this is not necessarily true for subdiffusive motion as has been observed in a number of recent papers [8–10]). More important for the current paper is that, for a finite time window, the resulting estimate of the MSD is still noisy. How these finite-size fluctuations affect the fluctuations of the motion parameters is the topic of our paper.

For a discretized trajectory $x_i^l = x^l(t + i\,\Delta t)$ with $i = 0, \ldots, M$ (sampling step Δt) and $l = 1, \ldots, d$ (where d is the number of spatial dimensions), this average of overlapping segments reads

$$\overline{\Delta R_t^2(\tau = k\,\Delta t)} = \frac{1}{M-k+1} \sum_{i=1}^{M-k+1} \sum_{l=1}^{d} \left(x_{i+k-1}^l - x_{i-1}^l\right)^2. \quad (3)$$

A local MSD is the same as Eq. (2), but the average is taken over a small local time window T for different values of the time increment τ. The resulting data are then reduced to pure numbers by dividing distances by a length scale ℓ, e.g., simply the length unit $\ell = 1\ \mu$m [for our choice of ℓ in our numerical examples, see below after Eq. (5)], and time by a reference time τ_0. The local MSD at m_τ different values (number of MSD points) of τ is then fitted to a power law,

$$\frac{\overline{\Delta R_t^2(\tau)}}{\ell^2} = A\left(\frac{\tau}{\tau_0}\right)^\alpha. \quad (4)$$

The exponent α carries information about the motion type [5]: $\alpha < 1$ implies subdiffusion, $\alpha \approx 1$ implies normal diffusion (Brownian motion), $\alpha > 1$ implies superdiffusion, and $\alpha \approx 2$ implies ballistic motion. The prefactor A has no physical dimension. The diffusion coefficient is directly proportional to the prefactor A. More specifically, if we set the time lag τ equal to the reference time τ_0, we obtain

$$D = \frac{\overline{\Delta R_t^2(\tau_0)}}{2\,d\tau_0} = \frac{A\ell^2}{2\,d\tau_0} = AD_0, \quad (5)$$

where d is the number of spatial dimensions and $D_0 = \ell^2/(2\,d\tau_0)$ is a parameter that carries the physical dimension of a diffusion coefficient and is set by our time and length scales. In the examples inspected below, we work with nondimensional units and set ℓ and Δt such that the numerical value of $D_0 = 1$. We also set the reference time τ_0 equal to the maximal lag time (i.e., $\tau_0 = m_\tau \Delta t$, where m_τ is the number of MSD points). For general applicability of our formulas, however, we keep D_0, ℓ, τ_0, and Δt in all formulas as free parameters.

The fit to the power law is performed by linear regression in a double logarithmic plot of the data. To this end, the m_τ pairs,

$$\left[\ln(k/m_\tau), \ln\left(\overline{\Delta R_t^2(k\,\Delta t)}/\ell^2\right)\right], \quad k = 1, \ldots, m_\tau \quad (6)$$

are fitted to

$$f(\ln(k/m_\tau)) = \ln A + \alpha\,\ln(k/m_\tau), \quad (7)$$

by the well-known formulas of linear regression [11] yielding the slope α and the prefactor $\ln A$ related to the diffusion coefficient by $A = D/D_0$ according to Eq. (5),

$$\alpha = \frac{\sum_k \ln\left(\overline{\Delta R_t^2(k\,\Delta t)}/\ell^2\right)\ln(k/m_\tau) - \frac{1}{m_\tau}\sum_{k,j}\ln\left(\overline{\Delta R_t^2(j\,\Delta t)}/\ell^2\right)\ln(k/m_\tau)}{\sum_k (\ln(k/m_\tau))^2 - \frac{1}{m_\tau}\left(\sum_k \ln(k/m_\tau)\right)^2}, \quad (8)$$

$$\ln A = \frac{1}{m_\tau}\sum_k \left[\ln\left(\overline{\Delta R_t^2(k\,\Delta t)}/\ell^2\right) - \alpha\ln\left(\frac{k}{m_\tau}\right)\right]. \quad (9)$$

Here, the index k (and also j) runs from $k = 1, \ldots, m_\tau$. Sliding the time window $T = M\,\Delta t$ over the entire trajectory [cf. Fig. 1(a)], the motion parameters $D(t)$ and $\alpha(t)$ can be extracted as functions of time. Because one uses a small time window T in order to obtain temporally local information, the resulting finite-size noise is not small, and consequently, $D(t)$ and $\alpha(t)$ will be stochastic processes, i.e., random functions of the time t as illustrated in Figs. 1(b) and 1(c).
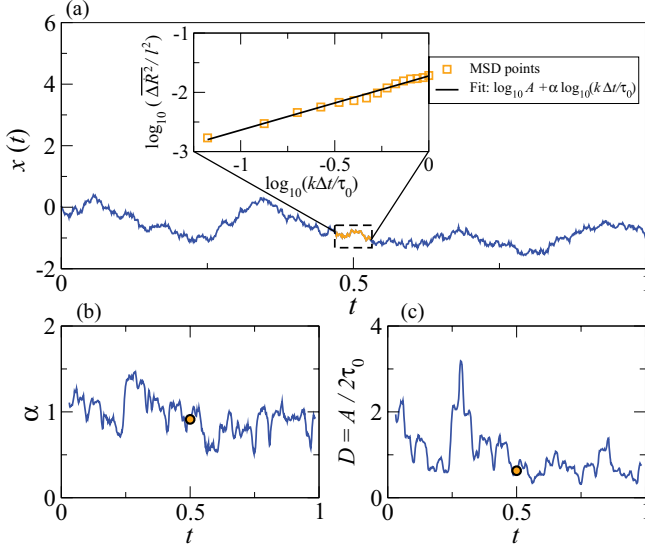
FIG. 1. (Color online) Illustration of the local MSD algorithm. (a) Trajectory of a Brownian particle is analyzed locally in a time window of M points (trajectory inside the dotted rectangle): The squared displacement for m_τ points is averaged over these M points and is fit by a linear relationship in log-log space [see inset of (a)]. The resulting slope (exponent) and intercept (proportional to the diffusion coefficient) are assigned to the midpoint of the window. By sliding the window over the trajectory, in this way, we obtain a time series of the exponent (b) and the diffusion coefficient (c). The circular dots in each (b) and (c) are the values obtained in (a). The trajectory is obtained using Eq. (10) for overdamped Brownian motion. Parameters used here are as follows: $m_\tau = 15$, $M = 60$, $\Delta t = 10^{-3}$, and $D = k_B T / \gamma = 1$.

The local-MSD algorithm has two parameters: M, the number of points in the time window and m_τ, the number of values of τ used in the power law fit. How M and m_τ influence the statistics of the estimated values of α and D is a question of foremost interest in our paper. For simple illustrations of our results, in this paper, we will exclusively consider the one-dimensional case. For the model introduced in the next section, the generalization of our analytical approximations to the multidimensional case is straightforward.

III. MODEL WITH PRESCRIBED VELOCITY FLUCTUATIONS

In our model, the dynamics of the displacement of a vesicle or bead is described by

$$\dot{x} = v, \tag{10}$$

where the velocity is assumed to be a stationary Gaussian stochastic process with vanishing mean value and correlation function,

$$\langle v(t)v(t+\tau)\rangle = C(\tau), \tag{11}$$

where $\langle\cdot\rangle$ denotes the ensemble average.

In discrete time [$x_i = x(i\,\Delta t)$ with time step Δt], a trajectory (sample path) of the process can be simulated by the simple map,

$$x_{i+1} = x_i + v_i \Delta t. \tag{12}$$

The correlation of the increments $v_i = [x_{i+1} - x_i]/\Delta t$ can be related to the continuous correlation function $C(\tau)$ as follows:

$$
\begin{aligned}
C_k &= \langle v_{i+k} v_i \rangle \\
&= \int_0^{\Delta t} d\tau [C((k-1)\Delta t + \tau) \\
&\quad + C((k+1)\Delta t - \tau)] \frac{\tau}{(\Delta t)^2}.
\end{aligned}
\tag{13}
$$

For a sufficiently small time step (within which the correlation function does not change much) but large k with $T = k\,\Delta t$, the integrand can be approximated by $2C(T)\tau/(\Delta t)^2$, and one obtains the intuitive result,

$$C_k \approx C(k\,\Delta t), \quad \Delta t \ll C(k\,\Delta t)/\dot{C}(k\,\Delta t). \tag{14}$$

In this limit, the discrete correlation agrees with the continuous correlation.

Traditionally, the time-continuous Eq. (10) with the correlation function Eq. (11) is regarded as the model to be considered. Equivalently, we can, however, consider the map Eq. (12) and the discrete correlation function as our starting point. This is practical in two respects. First, to simulate a sample path of the system, we need a temporal discretization in any case. Second, the velocity correlation might be obtainable from experimental data only in a discretized version, so typically, we know C_k but not $C(\tau)$. In this paper, we will solely use the discrete version as our starting point. We now discuss how to simulate sample paths and introduce two simple variants that are used as numerical examples.

We assumed above that the noise has Gaussian statistics. Under these circumstances, the velocity process can be simulated as an autoregressive (AR) process [11] as follows:

$$v_i = \sum_{k=1}^{p} d_k v_{i-k} + g_i, \tag{15}$$

where g_i are uncorrelated Gaussian random numbers with mean zero and variance σ_g^2. The coefficients d_k of this AR process can be obtained from the experimental incremental correlation function by the formula,

$$\mathbf{d} = \mathbf{P}^{-1} \mathbf{C} / \sigma_v^2, \tag{16}$$

where $\mathbf{d} = (d_1, d_2, \ldots, d_p)$ is the vector of unknown coefficients, $\mathbf{C} = (C_1, C_2, \ldots, C_p)$ is the vector of the discrete correlation function, and the matrix $\mathbf{P}$ is given by

$$
\mathbf{P} = \begin{bmatrix}
1 & \rho_1 & \rho_2 & \cdots & \rho_{p-1} \\
\rho_1 & 1 & \rho_1 & \cdots & \rho_{p-2} \\
\vdots & \vdots & \vdots & \cdots & \vdots \\
\rho_{p-1} & \rho_{p-2} & \rho_{p-3} & \cdots & 1
\end{bmatrix}, \tag{17}
$$

where

$$\rho_k = C_k / C_0 \tag{18}$$

is the normalized correlation coefficient.

The variance can be found from

$$\sigma_g^2 = C_0 - \sum_{k=1}^{p} d_k C_k. \tag{19}$$

Thus, for known σ_v^2, we can calculate σ_g^2.

We will consider two simple special cases in this paper. First, for uncorrelated velocity fluctuations, the map Eq. (12) is just the discrete version of overdamped Brownian motion [12],

$$C^{\text{WN}}(\tau) = 2\frac{k_B T}{\gamma}\delta(\tau) \ \rightarrow \ C_k^{\text{WN}} = 2\frac{k_B T}{\gamma\,\Delta t}\delta_{k,0} \quad (20)$$

[WN stands for white noise]. Here, k_B is the Boltzmann constant, T is temperature, and γ is the Stokes friction coefficient. In this case, all the coefficients d_k in Eq. (15) are zero, and the variance in the driving fluctuations reads

$$\langle v_i^2 \rangle = \langle g_i^2 \rangle = C_0 = 2\frac{k_B T}{\gamma\,\Delta t}. \quad (21)$$

For the white-noise case, the mean-square displacement is given by a pure diffusive law,

$$\langle \Delta x_k^2 \rangle := \langle (x_{i+k} - x_i)^2 \rangle = k(\Delta t)^2 C_0 = k\,\Delta t\frac{k_B T}{\gamma}. \quad (22)$$

In our second example, we will consider a finite discrete correlation that is negative at all finite lags and decays exponentially,

$$C_k^{\text{AP}} = (C_0 - C_1 e^{1/k_d})\delta_{k,0} + C_1 e^{-(k-1)/k_d}, \quad (23)$$

where, with $C_0 > 0$ and $C_1 < 0$, the correlations are the characteristics of an anti-persistent (AP) type of motion. Such

correlations have been recently observed experimentally for different kinds of organelles and particles [7,13]. We note that, on physical grounds, C_1 cannot take arbitrary values but has to obey

$$|C_1| \leqslant (e_1 C_0)/2, \quad (24)$$

where $e_1 = (1 - e^{-1/k_d})$. The exact mean-square displacement for this motion can be calculated [14] and reads

$$\langle \Delta x_k^2 \rangle = \Delta t^2 \left[k\left(C_0 + \frac{2C_1}{e_1} \right) - \frac{2C_1}{e_1^2}(1 - e^{-k/k_d}) \right]. \quad (25)$$

Interestingly, the MSD grows linearly with time at small times,

$$\langle \Delta x_k^2 \rangle_{\text{small}\,k} \approx k\,\Delta t^2 \left(C_0 + \frac{2C_1(e_1 - 1/k_d)}{e_1^2} \right), \quad (26)$$

and asymptotically at large times [as long as in Eq. (24) the equality does not hold],

$$\langle \Delta x_k^2 \rangle_{\text{large}\,k} \approx k\,\Delta t^2 \left(C_0 + \frac{2C_1}{e_1} \right). \quad (27)$$

In between these asymptotics, there exists a transition region characterized by a subdiffusive behavior [cf. Fig. 2(f)].
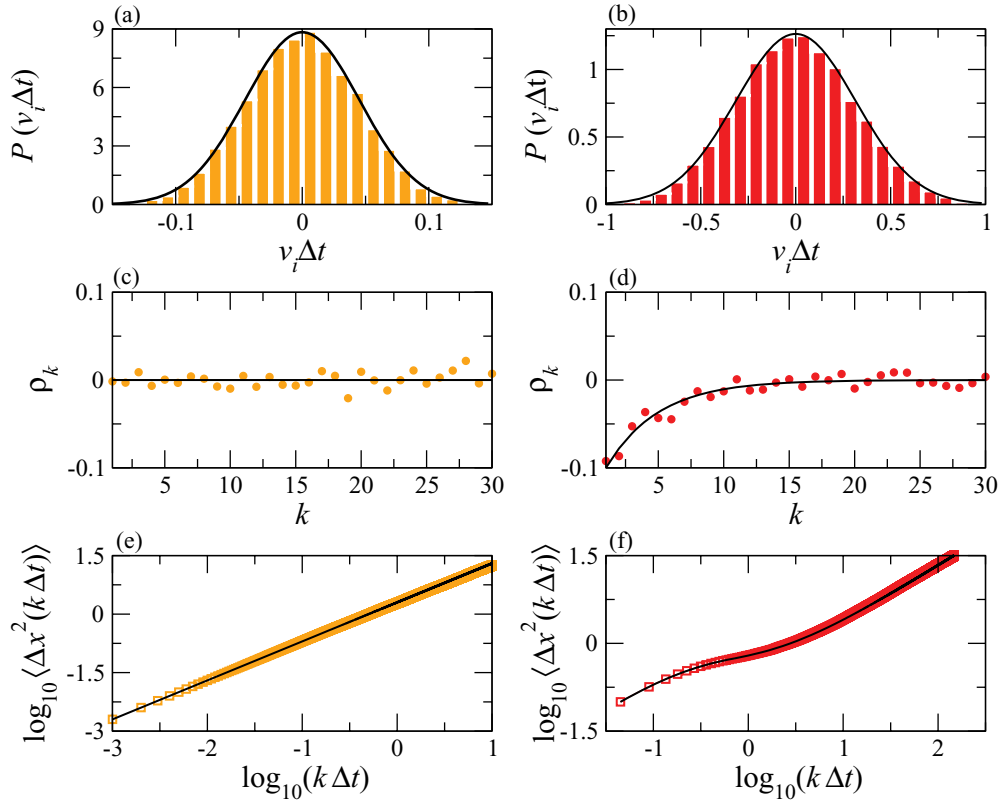

FIG. 2. (Color online) The statistics of the overdamped Brownian motion [(a), (c), and (e)] and antipersistent motion [(b), (d), and (f)] in discrete time. The probability density of the increments is Gaussian, as shown in (a) and (b) (the black lines are the corresponding fits). The normalized correlation functions of the increments are either δ correlated (overdamped Brownian motion) or negatively correlated at nonzero lag (antipersistent motion) as shown in (c) and (d), respectively (the zero-lag point is not shown); the line in (d) is the normalized form of Eq. (23). Panels (e) and (f) show the exact mean-square displacement of both velocity models for long times according to Eqs. (22) and (25); symbols are the results of numerical simulations with a large value of M (here, the algorithm is not local in time anymore). For both models, standard parameter values as given in Sec. IV B were used.

Assuming $k_d \gg 1$, the condition for this range reads

$$\varepsilon \frac{C_0}{|C_1|} \leqslant k \leqslant \frac{1/e_1}{\varepsilon[C_0 e_1/(2C_1) - 1]}, \qquad (28)$$

where ε is the relative deviation of the respective asymptotic expression from the exact result, e.g., for the small-k asymptotics,

$$\varepsilon = \frac{\langle \Delta x^2 \rangle_{\text{small } k} - \langle \Delta x^2 \rangle}{\langle \Delta x^2 \rangle} \ll 1. \qquad (29)$$

Simple Brownian motion is a special case with $C_1 = 0$ in which the two asymptotic regimes coincide and there is no transition region of subdiffusion. For finite negative correlations ($C_1 < 0$), the region of subdiffusion is not entirely determined by the correlation time of the increments $k_d \Delta t$, but also by the strength of the negative correlations, which is set by $2C_1/(e_1 C_0)$.

We emphasize that we consider a situation in which the full mean-square displacement is not considered because we have only a short (temporally local) sample of the particle's trajectory. Below, in Sec. V, we will compare the statistics to that of the full mean-square displacement curve.

IV. THE STATISTICS OF THE LOCAL MSD PARAMETERS

We know that the increments (estimates of the instantaneous velocity) are Gaussian distributed and that their linear correlation is given by the function C_k. The calculation of the statistics of a finite-size MSD (the square of a sum of correlated Gaussian variables or, more generally, a quadratic form) is a classical problem in the theory of stochastic processes (see Ref. [15] and references therein). However, what enters into the local MSD algorithm, in general, are sums over logarithms of such squared sums of Gaussian increments, i.e., a strongly nonlinear function of the simple Gaussian variables that we start with. Apart from special cases, it is difficult to calculate statistical distributions of such nonlinear functions of sums of Gaussians, and so, we are forced to use reasonable approximations. One such approximation for the case of only two MSD points but a large number of averaging points M will result in a Gaussian distribution of α and $\ln(D/D_0)$ [where, according to Eq. (5), $A = D/D_0$] because, in forming these numbers, we effectively add up many sufficiently independent random numbers, i.e., in the limit of large M, the central limit theorem applies. Under the assumption of a Gaussian distribution, it remains to calculate mean values and second-order moments (variances and covariances) of $\ln(D/D_0)$ and α. In the Appendix, this is performed in the general case of a correlated Gaussian velocity noise with discrete correlation function C_k. We obtain

$$\langle \alpha \rangle = 1 + \frac{\ln(1 + \rho_1)}{\ln 2}, \quad \langle \ln(D/D_0) \rangle = \ln\left[\frac{(C_0 + C_1)\Delta t}{2D_0}\right],$$

$$\sigma_\alpha^2 = \frac{s_1 + \rho_1^2 g_M^2 s_2 - 2\rho_1 g_M s_3}{[(C_0 + C_1)(M - 1)\ln 2]^2},$$

$$\sigma_{\ln(D/D_0)}^2 = \frac{s_1 + s_2 + 2s_3}{[(C_0 + C_1)(M - 1)]^2} - 1,$$

$$\sigma_{\alpha \ln(D/D_0)} = \frac{s_1 - \rho_1 g_M s_2 + (1 - \rho_1 g_M)s_3}{[(C_0 + C_1)(M - 1)]^2 \ln 2}, \qquad (30)$$

where $g_M = 1 - 1/M$ and we have further abbreviated

$$s_1 = M\left(C_0^2 + MC_1^2\right)g_M$$
$$+ 2\sum_{i=1}^{M-2}(M - i - 1)\left(C_i^2 + C_{i-1}C_{i+1}\right),$$

$$s_2 = M(M + 1)C_0^2 g_M + 4Mg_M\sum_{i=1}^{M-2}(M - i - 1)C_i^2, \quad (31)$$

$$s_3 = M(M - 2)C_0 C_1 g_M$$
$$+ 2\sum_{i=1}^{M-2}[2(M - i) - 1]C_{M-i-1}C_{M-i}.$$

Using these values, the Gaussian approximations of the joint probability density and the marginal densities are completely determined. They are given by

$$P(\alpha) = \frac{1}{\sqrt{2\pi\sigma_\alpha^2}}\exp\left[-\frac{(\alpha - \langle \alpha \rangle)^2}{2\sigma_\alpha^2}\right], \qquad (32)$$

$$P(D) = \frac{(D_0/D)}{\sqrt{2\pi\sigma_{\ln(D/D_0)}^2}}\exp\left[-\frac{[\ln(D/D_0) - \langle \ln(D/D_0) \rangle]^2}{2\sigma_{\ln(D/D_0)}^2}\right], \qquad (33)$$

$$P(D, \alpha) = \frac{\sqrt{4ab - c^2}}{2(D/D_0)\pi}\exp\left[-a(\ln(D/D_0) - \langle \ln(D/D_0) \rangle)^2 - b(\alpha - \langle \alpha \rangle)^2 - c(\alpha - \langle \alpha \rangle) \times (\ln(D/D_0) - \langle \ln(D/D_0) \rangle)\right]. \qquad (34)$$

The coefficients (a, b, c) appearing in Eq. (34) are derived using the first and second moments. In this paper, we plot $\hat{P}(\ln(D/D_0), \alpha)$ instead of $P(D, \alpha)$ because the former function is more symmetric with respect to its arguments,

$$\hat{P}(\ln(D/D_0), \alpha) = \frac{\sqrt{4ab - c^2}}{2\pi}\exp\left[-a(\ln(D/D_0) - \langle \ln(D/D_0) \rangle)^2 - b(\alpha - \langle \alpha \rangle)^2 - c(\alpha - \langle \alpha \rangle)(\ln(D/D_0) - \langle \ln(D/D_0) \rangle)\right]. \qquad (35)$$

In the following section, we discuss these formulas and compare them to numerical simulations for the two special cases (overdamped Brownian motion and antipersistent motion).

A. Results for an overdamped Brownian motion

The general formulas derived above reduce to quite simple expressions if the velocity is uncorrelated over a finite lag time ($C_k = 0$ for $k > 0$),

$$\langle \alpha \rangle = 1, \quad \langle \ln(D/D_0) \rangle = \ln\left(\frac{k_B T/\gamma}{D_0}\right), \qquad (36)$$

$$\sigma_\alpha^2 = \frac{1}{(M - 1)(\ln 2)^2}, \quad \sigma_{\ln(D/D_0)}^2 = \frac{3}{(M - 1)}, \qquad (37)$$

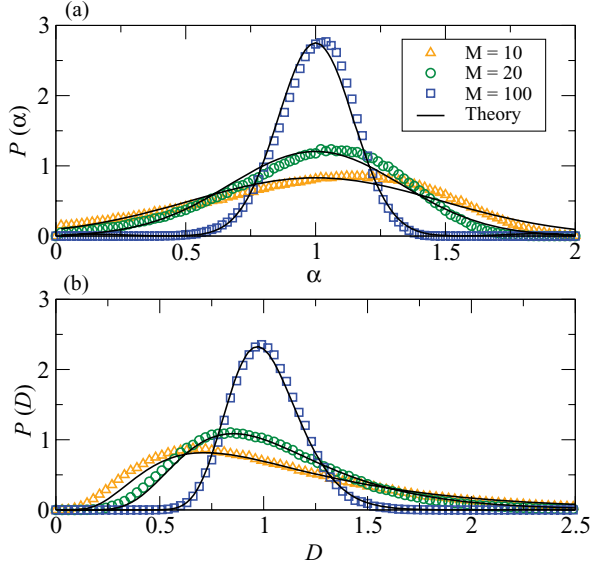$$\sigma_{\alpha \ln(D/D_0)} = \frac{1}{(M - 1)\ln 2}. \qquad (38)$$

FIG. 3. (Color online) Marginal distributions of (a) α and (b) D resulting from the local MSD algorithm for overdamped Brownian motion; data sets differ by the size of the rolling window as indicated. The number of local MSD points for all simulation data (symbols) is $m_\tau = 2$; theoretical approximations Eqs. (32) and (33) are shown by lines.

FIG. 4. (Color online) Joint distribution of α and $\ln A$ for an overdamped Brownian motion and two MSD points ($m_\tau = 2$): left column: simulation results compared to right column: theory Eq. (34) for various numbers of points of the rolling window as indicated.

The coefficients for the joint probability distribution are given by

$$a = \frac{(M-1)}{4}, \quad b = \frac{3(M-1)}{4}(\ln 2)^2, \quad c = -\frac{(M-1)}{2}\ln 2. \tag{39}$$

In the following, we set $D = k_B T/\gamma = 1$ in our simulations (this completely determines the physics of the process) and vary only the parameters of the local MSD algorithm. The time step for integration is taken as $\Delta t = 10^{-3}$. The analytical approximations for the first and second moments can be obtained from Eq. (30).

In Fig. 3, we compare the marginal distributions of α (a normal distribution) and D (a lognormal distribution) with numerical simulations. The quality of our approximation depends strongly on the number of points in the sliding window. Whereas, for $M = 10$, there is a finite discrepancy between simulation and theory, the agreement for $M = 100$ is very good. The values of α are equally distributed around the expected mean of 1, and the distribution of the estimated D is much more skewed, in particular, for smaller values of M.

In Fig. 4, we show the joint probability density of α and $\ln(D/D_0)$ for simulation data and analytical approximations side by side. According to our analytical calculation, this should be a two-dimensional Gaussian (corresponding to ellipsoid contour lines) with a clear correlation between the variables. The correlation is indeed evident for all values of M; the simulation data for $M = 10$, however, do not show the symmetry of a Gaussian (contour lines are not perfect ellipsoids). For larger M, the probability is confined to a
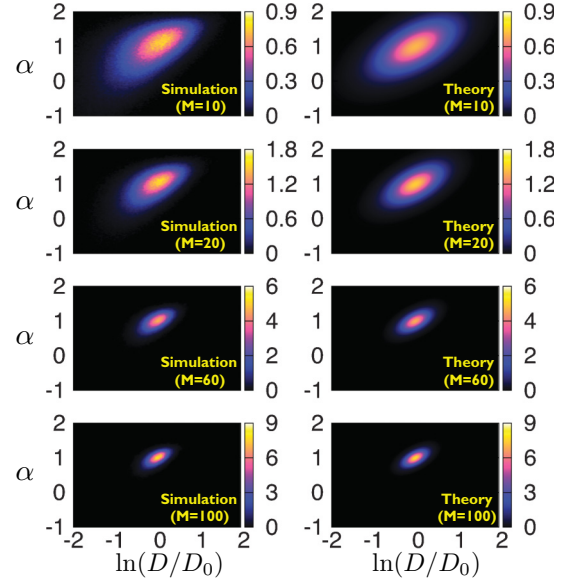
much smaller range of α and $\ln(D/D_0)$ but also becomes more symmetrically distributed.

Why do the two parameters show such a strong positive correlation? This could have the following reason. Consider all the points on the straight line (the true MSD curve in a double logarithmic plot) and then add an independent noise of equal amplitude to each point along the line. The intercept (corresponding to the diffusion coefficient) is given by the right-most point in the MSD curve (the MSD value at maximum lag time), and the exponent is given by the slope of the line. It is not hard to estimate that the resulting correlation between slope and intercept is positive. The value of this positive correlation, however, is much smaller than the correlation evident in the joint density. The strong positive correlation relies on the fact that the noise along the MSD curve is positively correlated, leading to an additional positive correlation in additive constant and slope.

Next, we discuss the marginal distributions as a function of the MSD points (Fig. 5); the number of points in the sliding time window is set to $M = 60$. One interesting question here is whether the variability of the estimated parameters decreases or increases if we take more than two MSD points into account. For once, every estimation of the MSD slope should become better by having more points. On the other hand, the points that we add are more noisy than the first two points, so our estimate should become more noisy. As apparent from the simulation results shown in Fig. 5, the latter effect dominates, and thus, the distributions (of both α and diffusion coefficient D) for larger numbers of MSD points are generally more variable than those for two MSD points.

Finally, we would like to directly compare the approximated mean values and standard deviations to those obtained by simulations of the overdamped Brownian motion. Mean values and standard deviations of (a) and (c) α and (b) and (d) D are
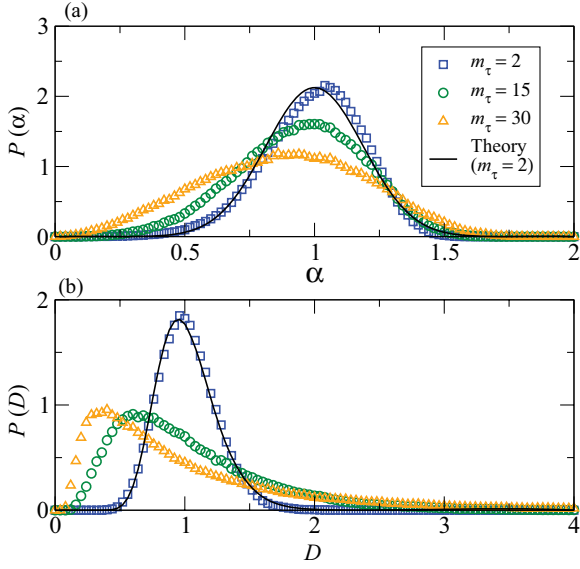
FIG. 5. (Color online) Marginal distributions of (a) α and (b) D resulting from the local MSD algorithm for overdamped Brownian motion. Data sets differ by the number of MSD points m_τ as indicated but have the same window size of $M = 60$ points.

discussed in Fig. 6 as functions of (a) and (b) the window size M and (c) and (d) the number of MSD points. Looking at mean α, we observe an underestimation of the true exponent of 1 for both small M and a large number of MSD points. At the same time, the variance in the α distribution drops

strongly with M. Furthermore, it undergoes a minimum if the number of MSD points is varied; this shallow minimum is attained at $m_\tau = 4$, and the minimum's value does not differ much from what we observe for two MSD points (the analytically tractable case). These observations indicate that a few tens of points in the rolling window and a small number of MSD points (preferably: 2) are recommendable for a reliable estimation of an overdamped Brownian motion's MSD exponent.

The results are for the mean and standard deviation of the diffusion coefficient's estimate point, although not as strongly, in the same direction. The mean of the diffusion coefficient does neither depend strongly on M nor on the number of MSD points. The standard deviation, however, drops strongly with M and increases with the number of MSD points. So, also for a reliable estimate of the diffusion coefficient, the case of large M and minimal number ($=2$) of MSD points seems to be optimal. This highlights the importance of the case that we are able to treat analytically.

B. Results for an antipersistent motion

Now, we tackle the more involved but interesting extension of a correlated velocity process with correlation function Eq. (23). Here, the increments are negatively correlated in qualitative accordance with recent experimental findings [7,13]. Our general result can be simplified for this specific correlation function because the parameters s_1, s_2, and s_3, which determine the variances and covariances of α, can be
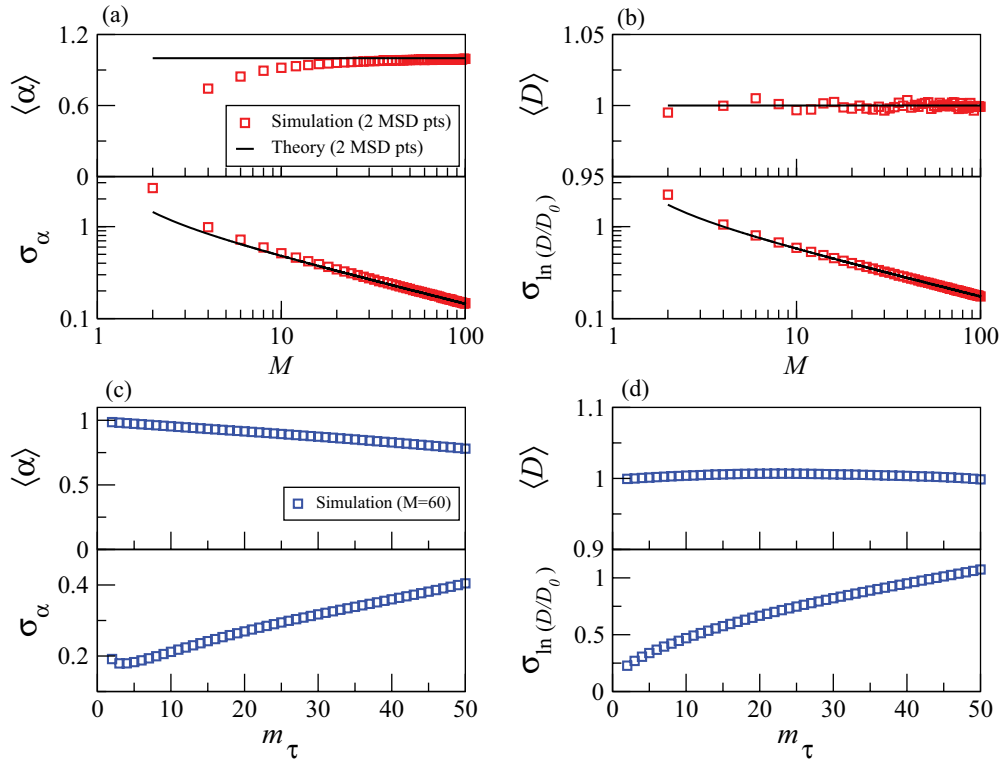

FIG. 6. (Color online) Mean values and standard deviations of (a) and (c) α and (b) and (d) $\ln A$ for the overdamped Brownian motion as functions of the (a) and (b) rolling window's size M and (c) and (d) the number of MSD points.

recast into the following forms:

$$s_1 = MC_0^2 + (M^2 + 3M - 2)C_1^2 + 2(M-1)C_0C_1e^{-1/k_d} + \frac{4C_1^2[e^{-2(M-2)/k_d} + (M-2)e^{2/k_d} - (M-1)]}{(e^{2/k_d} - 1)^2}, \tag{40}$$

$$s_2 = M(M+2)C_0^2 + \frac{4C_1^2e^{2/k_d}[e^{-2(M-1)/k_d} + (M-1)e^{2/k_d} - M]}{(e^{2/k_d} - 1)^2}, \tag{41}$$

$$s_3 = (M^2 + 3M - 2)C_0C_1 + 2C_1^2e^{3/k_d}\frac{[e^{-2(M-1)/k_d} + e^{-2M/k_d} + (1-2M)e^{-2/k_d} + (2M-3)]}{(e^{2/k_d} - 1)^2}. \tag{42}$$

Parameters of the correlation function are chosen as follows: $C_0 = 0.1/\Delta t^2$, $C_1 = -0.01/\Delta t^2$, and $k_d = 4$, yielding increment correlations similar to those observed experimentally in Ref. [7]. We choose the time step $\Delta t = 45 \times 10^{-3}$ such that the mean diffusion coefficient for $m_\tau = 2$ is unity.

In Fig. 7, we show marginal distributions of α and D for various sizes M of the rolling window. As in the white-noise case, the agreement with our theory becomes better for increasing M and is remarkably good for a time window of about $M = 100$ points. In general and as expected, both kinds of distributions become less variable when M is increased. However, in contrast to the case of overdamped Brownian motion (shown in Fig. 3), the mean value of α also depends strongly on the size of the window. In particular, the mean value for all M shown here is consistently lower than 1. This is an effect of the negative increment correlations.

For the joint distribution, we observe effects very similar to the white-noise case (see Fig. 8). The parameters α and $\ln(D/D_0)$ are positively correlated for the same reasons as discussed in the previous subsection. Furthermore, the joint density for small M shows some asymmetry that is inconsistent with our Gaussian approximation. This asymmetry becomes, however, less pronounced for increasing window size M.
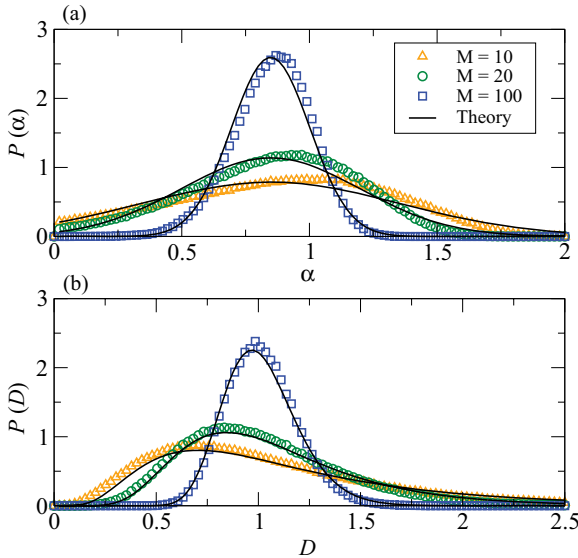
We turn again to the marginal distributions, inspecting now, by numerical simulation, the case of more than two MSD points (see Fig. 9). Clearly, as in the white-noise case, more than two MSD points increase the variability of the distributions. In marked contrast to the white-noise case, the number of MSD points also has a drastic effect on the estimated mean exponent of MSD growth and on the mean diffusion coefficient. Both decay strongly with increasing numbers of MSD points.

This aspect of the data becomes clearly visible in Fig. 10 where again, we show the mean values and standard deviations of α and D as functions of window size M and number of MSD points. The behavior of the standard deviation is similar to the white-noise case (cf. Fig. 6). However, the mean exponent's decay with the number of MSD points as well as its saturation for increasing M at a value below 1 is a clear consequence of the negative increment correlations and very different from what we observed for the overdamped Brownian motion.

The decrease in the mean exponent with an increasing number of MSD points is in line with the behavior of the exact MSD as a function of lag time: With increasing m_τ, we take more points from the subdiffusive transition region of the MSD curve into account and—being far away from the long-time asymptotic diffusive limit—this results in a drop in
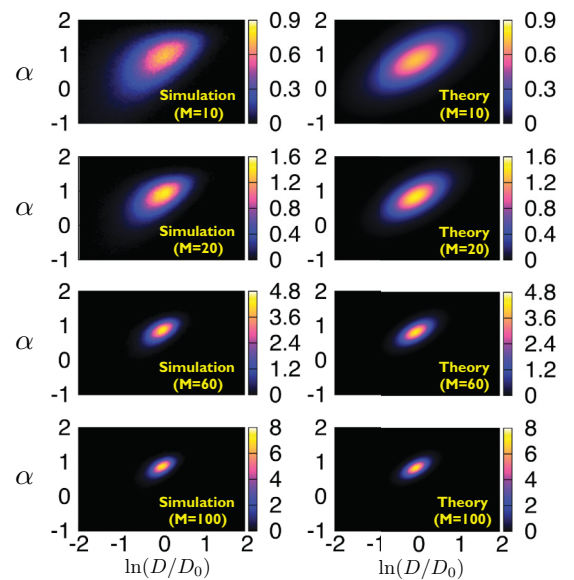
FIG. 7. (Color online) The marginal distributions of the MSD exponent α and the diffusion coefficient D for negatively correlated increments (antipersistent motion). Various sizes of the rolling time window are indicated; simulation and analytical results are shown by symbols and lines, respectively.

FIG. 8. (Color online) The joint distribution of α and $\ln A$ for various sizes M of the rolling window as indicated. Left column: simulation results and right column: theoretical prediction according to Eq. (34).
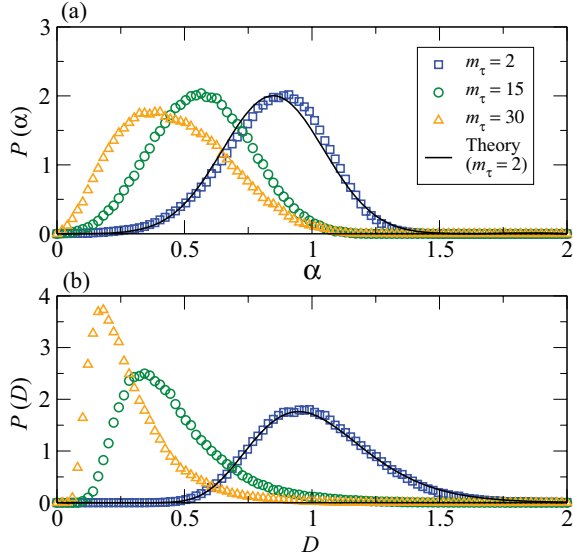
FIG. 9. (Color online) The marginal distributions of the MSD exponent α and the diffusion coefficient D for negatively correlated increments (antipersistent motion). Here, the number of MSD points is varied as indicated; theory is only plotted for $m_\tau = 2$.

the mean exponent as estimated by the local MSD analysis. With respect to this behavior, the question about the optimal m_τ is more complicated. From the statistical point of view, it is certainly recommendable, as in the case of overdamped Brownian motion, to choose a rather small number of MSD points. In order to catch the subdiffusive behavior, however,

one would rather favor a larger value of m_τ that yields a mean exponent more distinctly from 1. Looking at Fig. 10(c), a value with much smaller $\langle \alpha \rangle$ but still comparably small fluctuations would be given at about a quarter of M, here, $m_\tau = 15 = M/4$. This is also the value that has been used in different applications of the MSD analysis [1,7].

V. SUBDIFFUSION ON LONGER TIME SCALES FOR $M \to \infty$

So far, we have focused on small (local) time windows for the determination of the motion parameters α and D. This is relevant in the situation in which these parameters change over time as is the case, e.g., for the intracellular motion of vesicles. It is, however, instructive, to compare our results of the local MSD analysis to the exact MSD curve and its derivative for a long-time window ($M \to \infty$). We focus here solely on the exponent α in order to obtain some intuition for time scales for which this statistics reflects subdiffusional behavior. We reiterate that the situation considered in this section ($M \to \infty$) is not a common one in which one would apply the local MSD algorithm.

In the limit $M \to \infty$, the finite-size estimate of the MSD used in Eq. (8) becomes an exact average ($\overline{\Delta x^2} \to \langle \Delta x^2 \rangle$ as $M \to \infty$). In this limit, the value of α approaches the noiseless quantity,

$$\alpha_\infty = \frac{\sum_{k=1}^{m_\tau} \ln(\langle \Delta x_k^2 \rangle) \ln\left(\frac{k}{m_\tau}\right) - \frac{1}{m_\tau} \sum_{k,j=1}^{m_\tau} \ln(\langle \Delta x_j^2 \rangle) \ln\left(\frac{k}{m_\tau}\right)}{\sum_{k=1}^{m_\tau} \left[\ln\left(\frac{k}{m_\tau}\right)\right]^2 - \frac{1}{m_\tau}\left[\sum_{k,j=1}^{m_\tau} \ln\left(\frac{k}{m_\tau}\right)\right]^2}.$$

(43)

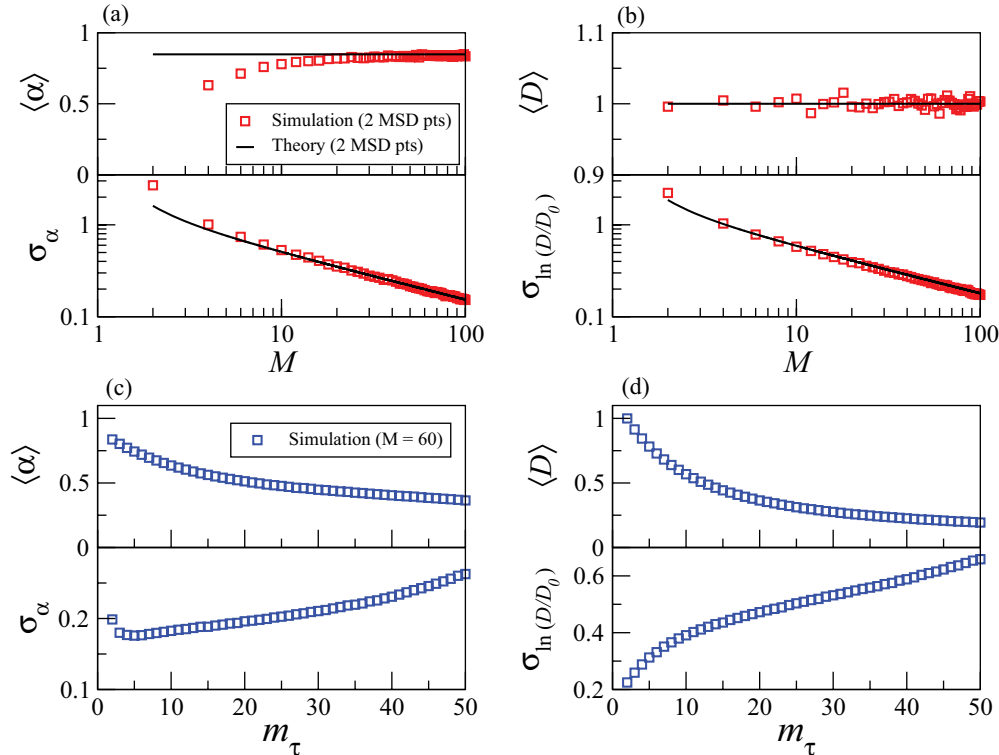FIG. 10. (Color online) Mean values and standard deviations of (a) and (c) α and (b) and (d) $\ln A$ for the antipersistent motion as functions of (a) and (b) the rolling window's size M and (c) and (d) the number of MSD points m_τ.

For the white-noise case, inserting the exact MSD according to Eq. (22) into Eq. (43) yields $\alpha_\infty = 1$ as can be expected. Hence, the deviations that are seen in Fig. 6(c) at large values of m_τ are due to the finite sample estimation of the MSD $\overline{\Delta x_k^2}$, i.e., the deviations become severe if m_τ does not differ much from M, here, for $M = 60$, this is true for $m_\tau \geqslant 20$. Before we discuss α_∞ for the correlated velocity process, we would like to recall the behavior of the exact MSD for this case.

In Fig. 11(a), we show the exact MSD according to Eq. (25) [this was already shown in Fig. 2(f)] together with the asymptotic results (dashed lines) for small and large k's, i.e., Eqs. (26) and (27), respectively. The range of subdiffusion is in agreement with Eq. (28) roughly given by $\log_{10} k\,\Delta t \in (-1.3, 1.3)$ (here, we used $\varepsilon = 0.1$) and coincides with the range for which the slope of the MSD curve [see Fig. 11(b), solid line] is significantly smaller than 1. The latter derivative attains a minimum and, in this way, indicates a most subdiffusive behavior that is determined by the temporal extension as well as by the strength of the negative correlations.

The function α_∞ for the correlated velocity process can be obtained by inserting the exact MSD Eq. (25) into Eq. (43). As shown in Fig. 11(c) by the green line, it also attains a minimum, although at a value of $m_\tau\,\Delta t$ that is larger than the time $k\,\Delta t$ at which the slope of the exact MSD becomes minimal. This is not surprising because Eq. (43) takes into account *all* MSD values *up to the maximal lag m_τ* (more specifically, it is a weighted sum of these values). In contrast, the derivative in the MSD-log-log plot takes into account only local features of the MSD curve. To better compare $\langle \alpha \rangle$ to the local slope of the MSD curve [solid line in Fig. 11(b)], we can associate α_∞ with the mean time scale of the whole window, which we may take approximately as *half* the maximum time. If we plot the α_∞ against $\log_{10}(m_\tau\,\Delta t/2)$ [dashed line in Fig. 11(b)], we obtain a curve with a minimum close to that of the derivative of the MSD. It is important that the time scale of maximal subdiffusion can be recovered by the algorithm in this way, provided the time window is long enough to cover the time range of sublinear MSD growth.

For finite values of M, we illustrate the finite-size noise effect of the numerically measured $\langle \alpha \rangle$ for $M = 60$ (blue line) and $M = 500$ (orange line). Both curves follow the exact mean value until they start deviating due to the effect of the finite-size estimation of the MSD. This illustrates that one cannot trust values of α that are determined for a number of MSD points only marginally smaller than the averaging window.

The results of this section also illustrate the simple point that we cannot extract subdiffusive behavior at time scales that are equal to or larger than the size of the averaging window. Still, the local MSD analysis already can show, for comparable small time windows, that the motion is qualitatively distinct from overdamped Brownian motion.

VI. SUMMARY AND CONCLUSIONS

In this paper, we have calculated the statistics of a local MSD algorithm in the special limit of two MSD points and a large averaging window. Our results for the joint and marginal probability densities revealed good agreement. Moreover,

further numerical simulations for larger numbers of MSD points indicated that the limit case we studied was important, giving, for our simple examples, the most reliable and unbiased mean values and the smallest variance in the distributions of MSD exponent and diffusion coefficient. However, we also discussed that a larger number of MSD points might be favorable to show a more distinct subdiffusive behavior of the motion.

In this paper, we also demonstrated how negative correlations between increments of the motion (antipersistent motion) yields subdiffusive behavior ($\alpha < 1$) on the small time scale of the local MSD algorithm. In the aforementioned special case of two MSD points, we could characterize this apparent subdiffusion analytically.

The case of antipersistent motion presented here shows transient subdiffusive behavior: At small and long time scales, the motion is diffusive. This is in contrast to persistent subdiffusion that has been observed previously in single cell tracking experiments with motion statistics similar to those of either a continuous time random walk (CTRW) [16,17] or a fractional Brownian motion (FBM) [13,17–19]. Identifying the underlying mechanism that leads to anomalous diffusion (CTRW or FBM) is an important open question and has been raised before in several papers wherein new trajectory analysis tools [20–22] were introduced to address this issue. The analysis presented in this paper does not address these questions.

Our results are interesting for applications in biological experiments in two respects. First of all, our results may be used to check the reliability of experimental estimates of the local MSD properties. For instance, one may discuss for which size of the rolling window it is meaningful to talk about subdiffusion once one observes mean exponents below 1. The results for the correlated Gaussian velocity process studied in this paper give orientation regarding this question.

Second, in comparing to the simple limit case of overdamped Brownian motion, experimentalists may distinguish how strongly the local MSD properties are influenced by the nonequilibrium environment of the cell. To this end, one may compare our simple formulas for the marginal densities for two MSD points to the statistics observed experimentally. In one specific example [7], this yielded the insight that the variability of the estimated parameters for intracellular data (motion of a bead internalized by *Dictyostelium discoideum* cells) is comparable to that obtained for simple Brownian motion, hence, this variability cannot be ascribed to specific biological properties of the cytoplasm in the living cell. Such conclusions may now also be possible for the study of intracellular motion in other cell types, such as neurons, cancer, and immune cells.

From a theoretical point of view, we have highlighted the importance of velocity correlations for the properties of the estimated MSD parameters. Besides more complicated models of subdiffusion, this suggests another class of Langevin-type models for the velocity that generates Gaussian fluctuations with correlations characteristic for an antipersistent motion, i.e., correlation functions with a pronounced negative tail. Although it is not complicated to generate higher-order Markov processes (i.e., an n-dimensional Ornstein-Uhlenbeck process) that is Gaussian and possesses such a correlation
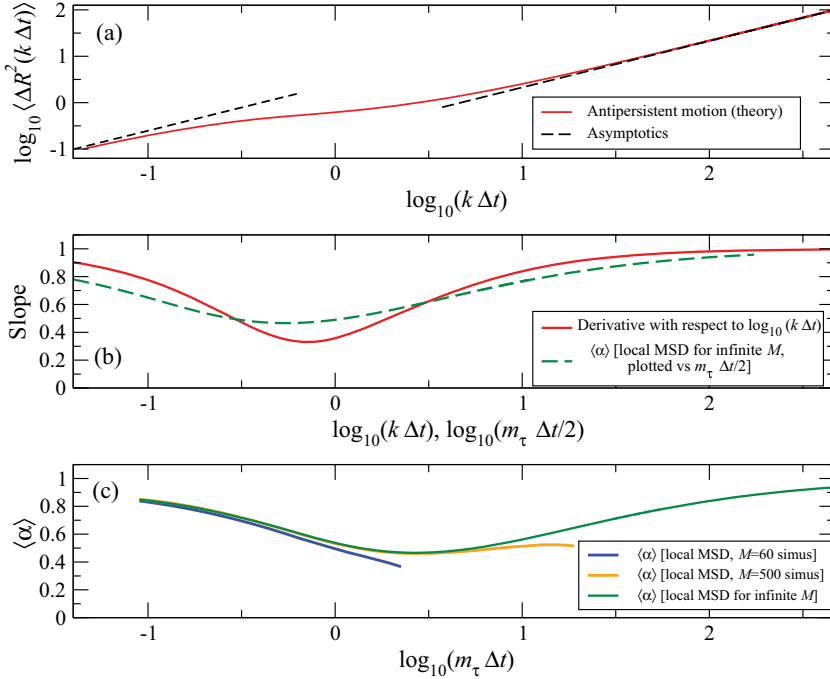
FIG. 11. (Color online) Comparison of the exact MSD, its derivative, and the mean value of α for $M \to \infty$. (a) Solid line: exact MSD Eq. (25) for the correlated velocity process and its asymptotic limits for small [Eq. (26)] and large times [Eq. (27)]. (b) Derivative of the MSD log-log plot, i.e., $d\,\log_{10}[\langle \Delta x^2(t) \rangle]/d\,\log_{10}(t)$ is compared to the mean value of α for $M \to \infty$ plotted vs the logarithm of half the maximal time window $\log_{10}(m_\tau\,\Delta t/2)$. (c) Mean value of α for various values of M as indicated vs maximal lag time $m_\tau\,\Delta t$.

function, relating such a model to the biophysical situation in the cell is still not fully understood (for a notable exception, see the recent Ref. [13]) and is certainly worth further study. Another unexplored venue is what kind of statistics the local-MSD algorithm yields for non-Gaussian velocity fluctuations, such as, for instance, in models of active Brownian motion [23] or coupled molecular motors [24], which have obvious significance for intracellular motility [25]. This leaves numerous exciting questions for future investigations.

APPENDIX: THE STATISTICS OF THE MOTION PARAMETER FOR TWO MSD POINTS ($m_\tau = 2$)

Substituting the expression for the discrete-time trajectory [Eq. (12) but in d dimensions] in the local-MSD algorithm [Eq. (3)], the estimate of the MSD, in terms of the velocity fluctuations, is given by

$$\overline{\Delta R_t^2(k\,\Delta t)} = \frac{\Delta t^2}{(M-k+1)} \sum_{i=1}^{M-k+1} \sum_{l=1}^{d} \left(\sum_{j=1}^{k} v_{i+j-1}^l \right)^2. \quad \text{(A1)}$$

Dividing by ℓ^2 and taking the logarithm on both sides, Eq. (A1) becomes

$$\ln\left(\frac{\overline{\Delta R_t^2(k\,\Delta t)}}{\ell^2} \right)$$
$$= \ln\left[\frac{\Delta t^2/\ell^2}{M-k+1} \sum_{i=1}^{M-k+1} \sum_{l=1}^{d} \left(\sum_{j=1}^{k} v_{i+j-1}^l \right)^2 \right]. \quad \text{(A2)}$$

For the special case of $d = 1$, Eq. (A2) becomes

$$\ln\left(\frac{\overline{\Delta x_t^2(k\,\Delta t)}}{\ell^2} \right) = \ln\left[\frac{\Delta t^2/\ell^2}{M-k+1} \sum_{i=1}^{M-k+1} \left(\sum_{j=1}^{k} v_{i+j-1} \right)^2 \right]. \quad \text{(A3)}$$

To determine the intercept $\ln A$ and slope α according to Eq. (7), we use the m_τ pairs $[\ln(k/m_\tau), \ln(\overline{\Delta R_t^2(k\,\Delta t)}/\ell^2)]$ in the formulas of linear regression, yielding Eqs. (8) and (9). The latter equations express the desired quantities in terms of a sum of logarithms of sums of correlated Gaussian variables. In other words, the statistics of $\ln A = \ln(D/D_0)$ and α is determined by highly nonlinear and lengthy functions of the Gaussian velocity fluctuations. It is, thus, generally quite difficult to relate the probability functions of α and D to those of the velocity fluctuations, in particular, if $m_\tau \geqslant 3$. However, for the case of two MSD points ($m_\tau = 2$), approximate analytical expressions for the marginal and joint distributions of α and D can be derived.

For two MSD points $m_\tau = 2$ and $d = 1$, using Eq. (8), the exponent α is given by

$$\alpha = \frac{1}{\ln 2}\left[\ln\left(\overline{\Delta x_t^2(2\,\Delta t)}/\ell^2 \right) - \ln\left(\overline{\Delta x_t^2(\Delta t)}/\ell^2 \right) \right]. \quad \text{(A4)}$$

Using Eq. (A3) in Eq. (8), this can be written as

$$\alpha = 1 + \frac{1}{\ln 2}\left[\ln\left(\frac{\Delta t^2/\ell^2}{2(M-1)} \sum_{i=1}^{M-1} (v_i + v_{i+1})^2 \right) \right.$$
$$\left. - \ln\left(\frac{\Delta t^2/\ell^2}{M} \sum_{i=1}^{M} v_i^2 \right) \right]. \quad \text{(A5)}$$

Similarly, using Eq. (A3) in Eq. (9), the diffusion coefficient is given by

$$\beta = \ln(D/D_0) = \ln\left(\frac{\overline{\Delta x_t^2(2\,\Delta t)}}{\ell^2}\right)$$

$$\equiv \ln 2 + \ln\left(\frac{\Delta t^2/\ell^2}{2(M-1)}\sum_{i=1}^{M-1}(v_i + v_{i+1})^2\right), \quad \text{(A6)}$$

where we use, in the following, β as a shortcut for the logarithm of the diffusion coefficient. Note that, in the special case

$m_\tau = 2$, the estimate of the diffusion coefficient (but not that of the exponent α) corresponds to a quadratic form of a Gaussian. For the latter problem, there exist alternative analytical methods to approximate the probability distribution (see, e.g., Ref. [15] and references therein) than presented in the following.

The arguments of the logarithms in Eqs. (A5) and (A6) are finite-size estimates of $C_0 = \langle v_i^2 \rangle$ and $C_0 + C_1$ (where the latter term was $C_1 = \langle v_i v_{i+1} \rangle$); deviations from the true mean values are expected to be small, and so, it is reasonable to expand the logarithms around these values, yielding

$$\ln\left(\frac{\Delta t^2/\ell^2}{M}\sum_{i=1}^{M}v_i^2\right) \approx \ln\left(\frac{C_0\Delta t^2}{\ell^2}\right) + \left(\frac{C_0^{-1}}{M}\sum_{i=1}^{M}v_i^2 - 1\right), \quad \text{(A7)}$$

$$\ln\left(\frac{\Delta t^2/\ell^2}{2(M-1)}\sum_{i=1}^{M-1}(v_i + v_{i+1})^2\right) \approx \ln\left(\frac{(C_0+C_1)\Delta t^2}{\ell^2}\right) + \left(\frac{(C_0+C_1)^{-1}}{2(M-1)}\sum_{i=1}^{M-1}(v_i + v_{i+1})^2 - 1\right). \quad \text{(A8)}$$

Equations (A5) and (A6) are then given as

$$\alpha = 1 + \frac{\ln(1+\rho_1)}{\ln 2} + \frac{(C_0+C_1)^{-1}}{\ln 2}\left(\frac{1}{2(M-1)}\sum_{i=1}^{M-1}\left(v_i^2 + v_{i+1}^2 + 2v_i v_{i+1}\right) - \frac{(1+\rho_1)}{M}\sum_{i=1}^{M}v_i^2\right), \quad \text{(A9)}$$

$$\beta = \ln\left[\frac{(C_0+C_1)\Delta t}{2D_0}\right] + \left(\frac{(C_0+C_1)^{-1}}{2(M-1)}\sum_{i=1}^{M-1}\left(v_i^2 + v_{i+1}^2 + 2v_i v_{i+1}\right)\right) - 1, \quad \text{(A10)}$$

where $\rho_1 = C_1/C_0$ is the correlation coefficient at lag 1. Using the fact that $\langle \sum_{i=1}^{M-1} v_i^2/(M-1)\rangle = C_0$ and $\langle \sum_{i=1}^{M-1} v_i v_{i+1}/(M-1)\rangle = C_1$, we obtain $\langle \alpha \rangle$ and $\langle \beta \rangle$ from Eqs. (A9) and (A10),

$$\langle \alpha \rangle = 1 + \frac{\ln(1+\rho_1)}{\ln 2}, \quad \text{(A11)}$$

$$\langle \beta \rangle = \ln\left[\frac{(C_0+C_1)\Delta t}{2D_0}\right]. \quad \text{(A12)}$$

We calculate the second-order moments using Eqs. (A9) and (A10) and Eqs. (A11) and (A12) and neglecting terms $\sim 1/M^2$. Defining $\sigma_\alpha^2 = \langle \alpha^2 \rangle - \langle \alpha \rangle^2$, $\sigma_{\ln(D/D_0)}^2 = \langle \beta^2 \rangle - \langle \beta \rangle^2$, $\sigma_{\alpha \ln(D/D_0)} = \langle (\alpha - \langle \alpha \rangle)(\beta - \langle \beta \rangle)\rangle$, and $g_M = (1 - 1/M)$, we obtain

$$\sigma_\alpha^2 \approx \frac{(C_0+C_1)^{-2}}{[(M-1)\ln 2]^2}\left[\left\langle\left(\sum_{i=1}^{M-1}v_i v_{i+1}\right)^2\right\rangle + \rho_1^2 g_M^2\left\langle\left(\sum_{i=1}^{M-1}v_i^2\right)^2\right\rangle - 2\rho_1 g_M\left\langle\sum_{i=1}^{M-1}v_i v_{i+1}\sum_{i=1}^{M-1}v_j^2\right\rangle\right], \quad \text{(A13)}$$

$$\sigma_{\ln(D/D_0)}^2 \approx \frac{(C_0+C_1)^{-2}}{(M-1)^2}\left[\left\langle\left(\sum_{i=1}^{M-1}v_i^2\right)^2\right\rangle + \left\langle\left(\sum_{i=1}^{M-1}v_i v_{i+1}\right)^2\right\rangle + 2\left\langle\sum_{i=1}^{M-1}v_i v_{i+1}\sum_{i=1}^{M-1}v_j^2\right\rangle\right] - 1, \quad \text{(A14)}$$

$$\sigma_{\alpha \ln(D/D_0)} \approx \frac{(C_0+C_1)^{-2}}{(M-1)^2\ln 2}\left[\left\langle\left(\sum_{i=1}^{M}v_i v_{i+1}\right)^2\right\rangle - \rho_1 g_M\left\langle\left(\sum_{i=1}^{M-1}v_i^2\right)^2\right\rangle + (1-\rho_1 g_M)\left\langle\sum_{i=1}^{M-1}v_i v_{i+1}\sum_{i=1}^{M-1}v_j^2\right\rangle\right]. \quad \text{(A15)}$$

Equations (A13)–(A15) involve fourth-order moments, which can be simplified for Gaussian distributed random numbers by expressing them by second-order moments as follows [26]:

$$\langle A_1 A_2 A_3 A_4 \rangle = \langle A_1 A_2 \rangle\langle A_3 A_4 \rangle + \langle A_1 A_3 \rangle\langle A_2 A_4 \rangle + \langle A_1 A_4 \rangle\langle A_2 A_3 \rangle. \quad \text{(A16)}$$

After some algebraic manipulations, this yields, for the sums of velocity products in Eqs. (A13)–(A15),

$$s_1 = \left\langle \left(\sum_{i=1}^{M-1} v_i v_{i+1} \right)^2 \right\rangle = M(C_0^2 + MC_1^2)g_M + 2\sum_{i=1}^{M-2}(M-i-1)\left(C_i^2 + C_{i-1}C_{i+1}\right), \tag{A17}$$

$$s_2 = \left\langle \left(\sum_{i=1}^{M-1} v_i^2 \right)^2 \right\rangle = M(M+1)C_0^2 g_M + 4Mg_M \sum_{i=1}^{M-2}(M-i-1)C_i^2, \tag{A18}$$

$$s_3 = \left\langle \sum_{i=1}^{M-1} v_i v_{i+1} \sum_{i=1}^{M-1} v_j^2 \right\rangle = M(M-2)C_0 C_1 g_M + 2\sum_{i=1}^{M-2}[2(M-i)-1]C_{M-i-1}C_{M-i}. \tag{A19}$$

Using these expressions in Eqs. (A13)–(A15), we obtain the expressions for variances and covariances stated in the main text, Eqs. (30). It is straightforward to extract, from mean values, variances, and covariances, the parameters of a two-dimensional Gaussian. For coefficients (a,b,c), we make the simplifying assumption that $g_M \approx 1$, which is justified for a sufficiently large window size. This yields

$$a \approx -\frac{1}{2}\frac{M^2\left(C_0^2 s_1 + C_1^2 s_2 - 2C_0 C_1 s_3\right)}{M^2\left(C_0^2 s_1 + C_1^2 s_2 - 2C_0 C_1 s_3\right) - s_1 s_2 + s_3^2}, \tag{A20}$$

$$b \approx \frac{1}{2}\frac{(MC_0 \ln 2)^2[M^2(C_0 + C_1)^2 - (s_1 + s_2 + 2s_3)]}{M^2\left(C_0^2 s_1 + C_1^2 s_2 - 2C_0 C_1 s_3\right) - s_1 s_2 + s_3^2}, \tag{A21}$$

$$c \approx \frac{M^2 C_0 \ln 2[C_0 s_1 - C_1 s_2 + (C_0 - C_1)s_3]}{M^2\left(C_0^2 s_1 + C_1^2 s_2 - 2C_0 C_1 s_3\right) - s_1 s_2 + s_3^2}. \tag{A22}$$

[1] D. Arcizet, B. Meier, E. Sackmann, J. O. Rädler, and D. Heinrich, Phys. Rev. Lett. **101**, 248103 (2008).

[2] J. Mahowald, D. Arcizet, and D. Heinrich, ChemPhysChem **10**, 1559 (2009).

[3] C. Loverdo, O. Benichou, M. Moreau, and R. Voituriez, Nat. Phys. **4**, 134 (2008).

[4] C. P. Brangwynne, G. H. Koenderink, F. C. MacKintosh, and D. A. Weitz, Trends Cell Biol. **19**, 423 (2009).

[5] R. Metzler and J. Klafter, Phys. Rep. **330**, 1 (2000).

[6] J. P. Bouchad and A. Georges, Phys. Rep. **195**, 127 (1990).

[7] M. Otten, A. Nandi, D. Arcizet, M. Goreslashvili, B. Lindner, and D. Heinrich, Biophys. J. **102**, 758 (2012).

[8] Y. He, S. Burov, R. Metzler, and E. Barkai, Phys. Rev. Lett. **101**, 058101 (2008).

[9] A. Lubelski, I. M. Sokolov, and J. Klafter, Phys. Rev. Lett. **100**, 250602 (2008).

[10] S. Burov, J. H. Jeon, R. Metzler, and E. Barkai, Phys. Chem. Chem. Phys. **13**, 1800 (2011).

[11] G. E. P. Box, G. M. Jenkins, and G. C. Reinsel, *Time Series Analysis: Forecasting and Control* (Prentice-Hall, Englewood Cliffs, NJ, 1994).

[12] H. Risken, *The Fokker-Planck Equation* (Springer, Berlin, 1984).

[13] S. C. Weber, A. J. Spakowitz, and J. A. Theriot, Phys. Rev. Lett. **104**, 238102 (2010).

[14] The mean-square displacement can be written as $\langle \Delta x_t^2(N \Delta t) \rangle = \Delta t^2 \sum_{i=1}^N \sum_{j=1}^N \langle v_i v_j \rangle = C_0 \Delta t^2[N + 2\sum_{k=1}^{N-1} \rho_k(N-k)]$. Insertion of the correlation function yields Eq. (25).

[15] D. S. Grebenkov, Phys. Rev. E **84**, 031124 (2011).

[16] A. V. Weigel, B. Simon, M. M. Tamkun, and D. Krapf, Proc. Natl. Acad. Sci. USA **108**, 6438 (2011).

[17] J.-H. Jeon, V. Tejedor, S. Burov, E. Barkai, C. Selhuber-Unkel, K. Berg-Sørensen, L. Oddershede, and R. Metzler, Phys. Rev. Lett. **106**, 048103 (2011).

[18] I. Y. Wong, M. L. Gardel, D. R. Reichman, E. R. Weeks, M. T. Valentine, A. R. Bausch, and D. A. Weitz, Phys. Rev. Lett. **92**, 178101 (2004).

[19] J. Szymanski and M. Weiss, Phys. Rev. Lett. **103**, 038102 (2009).

[20] V. Tejedor *et al.*, Biophys. J. **98**, 1364 (2010).

[21] M. Magdziarz, A. Weron, K. Burnecki, and J. Klafter, Phys. Rev. Lett. **103**, 180602 (2009).

[22] M. Bauer, R. Valiullin, G. Radons, and J. Kärger, J. Chem. Phys. **135**, 144118 (2011).

[23] B. Lindner, New J. Phys. **9**, 136 (2007).

[24] B. Lindner and E. M. Nicola, Phys. Rev. Lett. **101**, 190603 (2008).

[25] A. Caspi, R. Granek, and M. Elbaum, Phys. Rev. Lett. **85**, 5655 (2000).

[26] C. W. Gardiner, *Handbook of Stochastic Methods* (Springer-Verlag, Berlin, 1985).